Signal propagation in nonlinear optical fibers

Michelle De Decker, José María García Roldán,
James Herterich, Alexander Kospach, Tommaso Ristori
Instructor: Luigi Barletti

June 21, 2011

1 Introduction

Optical fibers made of pure glass (silica) are used as a medium for telecommunication and networking as they act as waveguides to transmit light between the two fiber ends. The information carrying signal travels for hundreds, or even thousands, of kilometers (see Fig 1) and undergoes several degeneration processes. Further undersired noise enters the system due to the fact that the signal needs to be periodically reinforced by optical amplifiers over its long journey (see Fig 2).

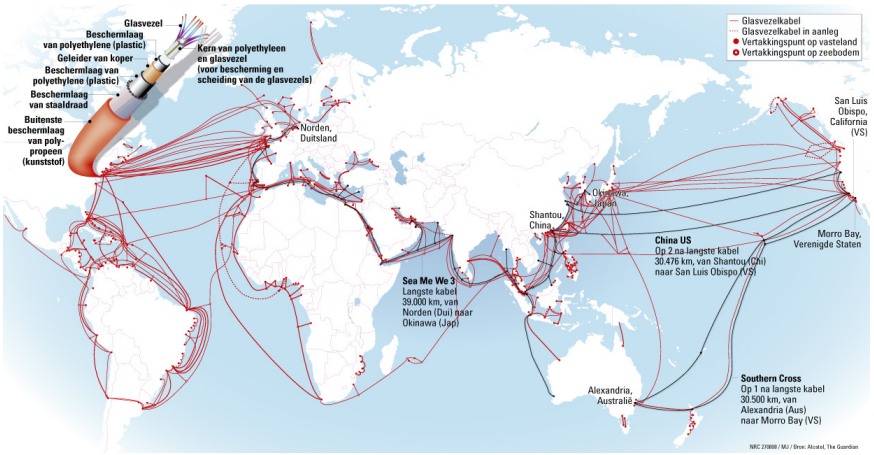

Figure 1: Optical fibers carry informations for hundreds, or even thousands, of kilometers.

Modelling and simulation of the signal and the degeneration processes is fundamental for the correct interpretation of the output signal and is, therefore, of central interest for the telecommunications industries. Degeneration processes include chromatic dispersion (different wavelenghts travel with different speed), nonlinear self-phase modulation (Kerr effect) and dissipation. Furthermore the signal and noise is nonlinearly mix up during the propagation, and this contributes to the degeneration of the output. All these phenomena can be described by a one-dimensional, nonlinear Schrödinger equation, with stochastic input data.

Our purpose is to investigate the propagation of the electromagnetic signal by exploiting the Madelung transform which reduces the one-dimensional Schrödinger equation to an Euler-like system of equations for a compressible fluid. This allows to deduce an approximated "semiclassical" model which can more easily handled for numerical simulations and which is more treatable when the stochastic data are considered.

An optical fiber is made of three components: the jacket, cladding and the core. For a cross-sectional image of a fiber see Fig 3(a). The refraction index gradient between core and cladding

Figure 2: Noise is mixed into the signal as the signal is reinforced at every amplifier along its path.

acts as a confinement trap for the electromagnetic wave in the transverse directions (xy). The propagating part of the electromagnetic wave is along the z (longitudinal) direction (into the page) within the core. This is the important part to be analyzed for our purposes. For our problem we will consider a single-mode fiber which means that the electromagnetic wave in the xy (transverse) directions has a stationary shape (called a *mode*). Usually $a \sim 5$ m and $b \sim 50$ m, for a standard single-mode fiber. In Fig 3(b) we can see different fiber modes.

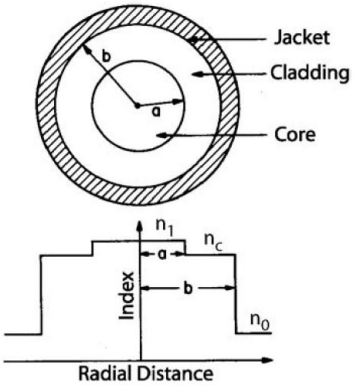

(a) Cross section

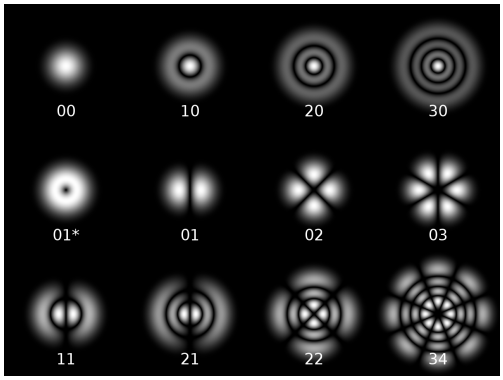

(b) Transverse modes

Figure 3: A single-mode optical fiber.

This report is arranged as follows: In section 2 the electromagnetic field within the optical fiber and the nonlinear Schr odinger equation (NLSE) for the modulation of the electromagnetic field are defined. In section 3 we introduce new variables to nondimensionalize the problem and a simplied fluid model is found with the use of the Madelung transform. In section 4 we report our solutions. We do a brief introduction to adding the stochasic noise to the input data in section 5 and finally our conclusions are summarized in section 6.

2 The matematical problem

The electromagnetic field inside the fiber can be assumed to have this form:

$$\vec{E}(x,y,z,T) = F(x,y)e^{i(\beta_0 z - \omega_0 T)}U(z,T)\vec{\nu} \tag{1}$$

where $F(x,y)$ is the transverse mode (assumed to be fixed), $e^{i(\beta_0 z-\omega_0 T)}$ is the longitudinal carrier wave, $U(z,T)$ is the longitudinal modulation and $\vec{\nu}$ polarization vector (assumed to be fixed). The modulation $U(z,T)$ is that component which carries the information and so is the function of interest here. In general, the propagation can be described by the nonlinear Schrödinger equation with cubic nonlinearity, where the roles of space and time variables are inverted with respect to

the usual Schrödinger equation of quantum mechanics:

$$iU_z = -i\beta_1 U_T - \frac{\beta_2}{2} U_{TT} - i\alpha U + \gamma |U|^2 U. \tag{2}$$

Here, the four terms on the right hand side are defined as the wave packet drift, chromatic dispersion (CD), dissipation and the self-phase modulation (SPM) terms. The drift term can be neglected by introducing a new time variable,

$$t = T - \beta_1 z. \tag{3}$$

So clocks along the fiber are set to $t = 0$ at the arrival of the pulse center (traveling at the group

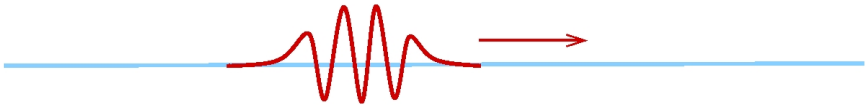

Figure 4: Drift of the wave packet.

velocity $1/\beta_1$, see Fig 4). Now the new modulation can be expressed as

$$u(z,t) = U(z, t + \beta_1 z) \tag{4}$$

and it obeys the NLSE

$$iu_z = -\frac{\beta_2}{2} u_{tt} - i\alpha u + \gamma |u|^2 u \tag{5}$$

which, from now on, will be our model of signal propagation in a nonlinear optical fiber. This has to be supplemented with input conditions at $z = 0$:

$$u(0,t) = u_0(t). \tag{6}$$

Later we will consider stochastic input data.

3 Rescaling

We nondimensionalize the problem by introducting new variables

$$t = t_0 \hat{t}, \quad z = z_0 \hat{z}, \quad u = u_0 \hat{u}, \tag{7}$$

where t_0, z_0 and u_0^2 are reference time, length and power, while the hatted terms are the new dimensionless variables. Furthermore we define

$$P_0 = u_0^2, \quad N_D = \frac{t_0^2}{\beta_2}, \quad N_{NL} = \frac{1}{\gamma P_0}. \tag{8}$$

Substituting these into equation (5) and dropping the hat notation we get

$$i\frac{N_{NL}}{z_0} u_z = -\frac{N_{NL}}{2N_D} u_{tt} + |u|^2 u - \frac{i\alpha}{2} N_{NL} u \tag{9}$$

In order to get the "semiclassical" scaling,[1] it is convienient to set $\epsilon^2 = \frac{N_{NL}}{N_D}$ and then we choose z_0 such that $\epsilon = \frac{N_{NL}}{z_0}$. We want ϵ to be a small parameter, so that later when we take the Madelung

[1] The term *semiclassical* is used in analogy with the semiclassical scaling of the Schrödinger equation of quantum mechanics but, of course, here the scaling has a different meaning, namely that of SPM being much stronger than CD.

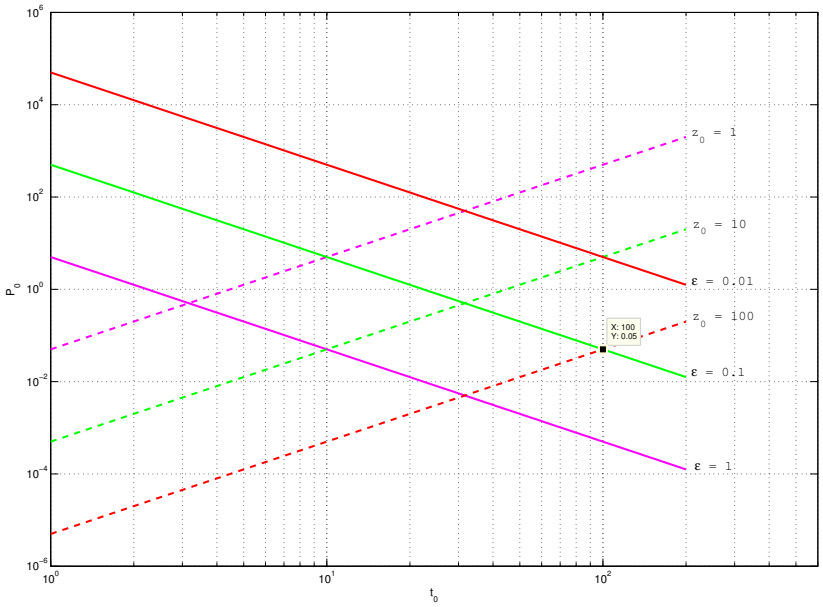

Figure 5: Plot of equations (12) and (13)

transformation we may neglect part of the nonlinearity in the equation. To ensure ϵ is small we choose appropriate values for t_0 and P_0. From the definitions of ϵ we may express the typical length scale as

$$z_0 = \sqrt{N_{NL} N_D}, \tag{10}$$

and the the NLSE can be written in the following "semiclassical" scaled form

$$i\epsilon u_z = -\frac{\epsilon^2}{2} u_{tt} + |u|^2 u - \frac{i\alpha}{2} N_{NL} u. \tag{11}$$

To find a small ϵ value that corresponds to a large z_0 value we plot the two graphs (see Fig 6)

$$P_0 = \frac{t_0^2}{\gamma \beta z_0^2}, \tag{12}$$

$$P_0 = \frac{\beta}{\epsilon^2 \gamma t_0^2}, \tag{13}$$

for different (logarithmically spaced) values of ϵ and z_0. Looking at where the graphs intersect we may choose appropriate ranges for t_0 and P_0. We choose $t_0 \approx 100$ ps and $P_0 \approx 50$ mW. Other parameters, such as

$$\alpha = 0.02\ km^{-1}, \qquad \beta = 10\ ps^2 km^{-1}, \qquad \gamma = 2\ W^{-1} km^{-1},$$

are fixed as they are physical properties of the fiber and the typical values are taken from literature. The other parameter values turn out to be

$$\epsilon = 0.1, \qquad z_0 = 100\ km, \qquad \hat{\alpha} = \alpha z_0 = 2, \qquad N_{NL} = 10\ km, \qquad N_D = 1000\ km.$$

We then apply the Madelung transform to (11) which assumes $u(z,t)$ to have the form

$$u(z,t) = \sqrt{\rho(z,t)}\, \exp\left(\frac{i}{\epsilon}\phi(z,t)\right), \tag{14}$$

$$J(z,t) = \phi_t(z,t), \tag{15}$$

where ρ may be interpreted as the amplitude of the propagation and ϕ is the phase. Substituting these expressions into (11) we obtain two real equations of a fluid-dynamic form:

$$\rho_z + (\rho J)_t = -\hat{\alpha}\rho, \tag{16a}$$

$$J_z + \frac{\partial}{\partial t}\left[\frac{J^2}{2} + \rho - \epsilon^2\left(\frac{\rho_{tt}}{4\rho} - \frac{\rho_t^2}{8\rho^2}\right)\right] = 0. \tag{16b}$$

These are called the Madelung equations. By neglecting the $\mathcal{O}(\epsilon^2)$ terms we finally obtain a simplified fluid model to work with:

$$\rho_z + (\rho J)_t = -\hat{\alpha}\rho, \tag{17a}$$

$$J_z + \frac{\partial}{\partial t}\left(\frac{J^2}{2} + \rho\right) = 0. \tag{17b}$$

In the following section these simplified equations will be solved numerically using COMSOL Multiphysics® with suitable initial data and boundary conditions. To investigate the effect of neglecting the nonlinear term a comparison of the approximate solution with the result obtained with the full NLSE will be made.

4 Solutions

In this section we will implement both the simplied fluid model in (17) and the full NLSE using the numerical package COMSOL Multiphysics® which makes use of the finite element method. The reduced fluid model is easier to implement numerically and when including the effect of stochastic input data (details to follow later) the fluid model is simplier to work with. Then we will compare the simulations obtained with the simplified fluid model with those obtained with the full NLSE to demonstrate that the main trend of the solutions are captured.

Our problem does not have natural boundary conditions, but when implementing the problem in COMSOL we are required to stipulate boundary conditions. To avoid this complication we choose a domain much larger than the pulse width and define trival Neumann boundary conditions at a distance far enough away from the region of interest. This way the effect of the boundary condition on the solution is negligible. So the initial condition will have a dominating effect on the solution, and so we will explore many different initial deterministic data inputs, such as Gaussian Pulses, Chirped Gaussian Pulses, Super Gaussian Pulses and Hyperbolic Secant Pulses. A typical length for the pulse width is $2\sigma t_0$, where σ is the standard deviation of the initial data, so the domain chosen for the solution is $t \in [-10t_0, 10t_0]$.

4.1 Gaussian Pulses

To start with we solve the problem using a Gaussian pulse for the initial data, defined as

$$u(0,t) = \exp\left(-\frac{t^2}{2\sigma^2}\right), \tag{18}$$

which corresponds to initial conditions for the fluid system (17),

$$\begin{aligned} \rho(0,t) &= \exp\left(-\frac{t^2}{\sigma^2}\right), \\ J(0,t) &= 0. \end{aligned}$$

As seen in Figs 6(a) and 6(b), where the fluid model and the full NLSE solutions are represented respectively, we have excellent agreement even though $\epsilon = 0.1$ is not particularly small.

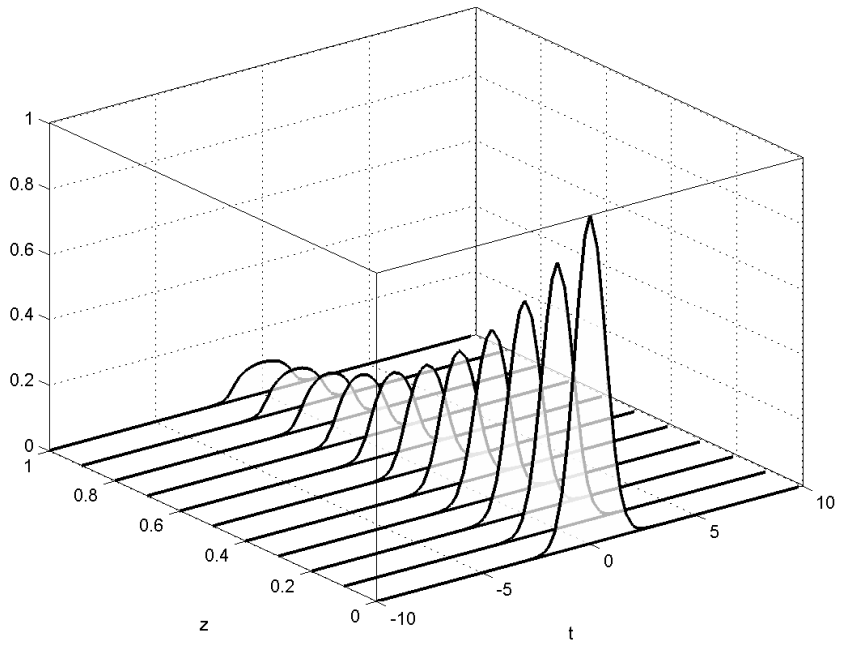

(a) The fluid model solution.

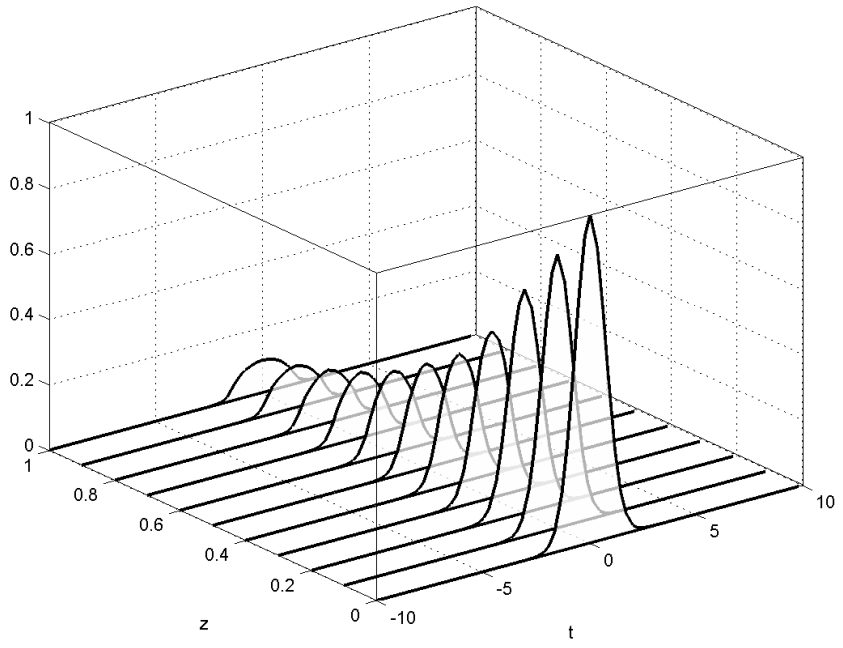

(b) The full NLSE solution.

Figure 6: A comparison of the fluid model solution (a) of the fluid equations (17) with the full NLSE (b) using a Gaussian Pulse for initial condition.

4.2 Chirped Gaussian Pulses

Now we work with a chirped intial condition, i.e. the initial conditional has a frequency that varies in time where c is the chirped parameter, defined as

$$u(0,t) = \exp\left(-\frac{(1+ic)t^2}{2\sigma^2}\right) \tag{19}$$

which corresponds to initial conditions for the fluid system (17),

$$\begin{aligned} \rho(0,t) &= \exp\left(-\frac{t^2}{\sigma^2}\right), \\ J(0,t) &= -\frac{c\epsilon t}{\sigma^2}. \end{aligned}$$

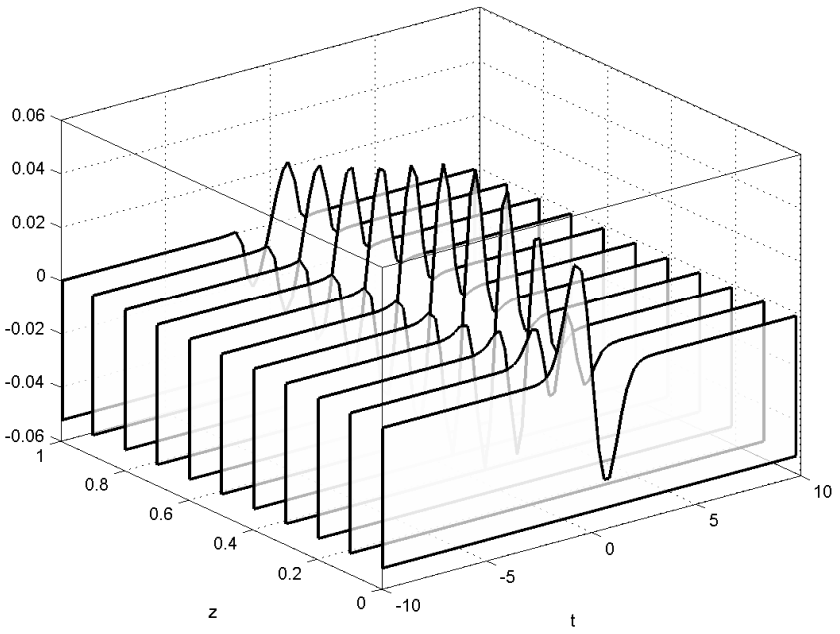

(a) Approximate solution.

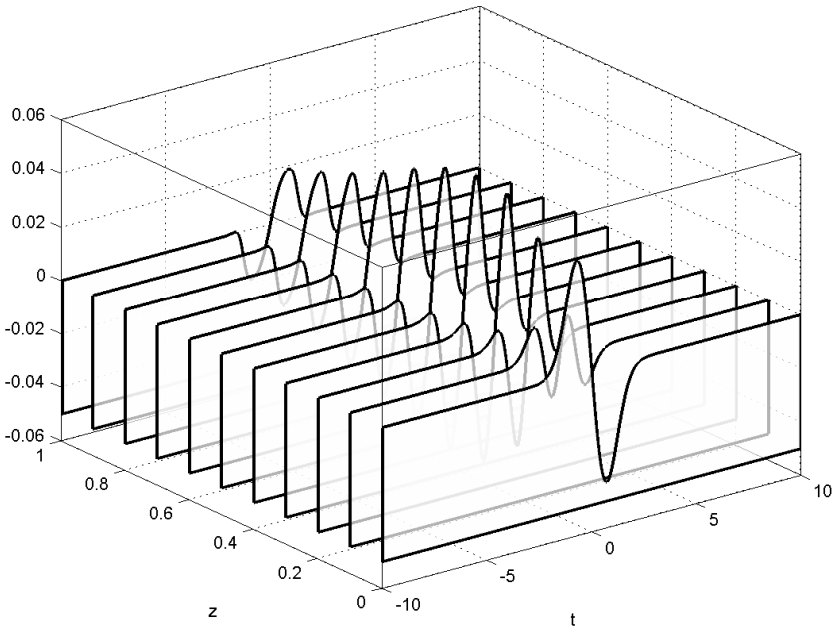

(b) Full solution.

Figure 7: A comparison of ρJ of the fluid model (a) with the full NLSE (b) using a Chirped Gaussian Pulse with $c = 1$ for initial condition.

In the case of non-vanishing initial chirp c we show the graph of ρJ because ρ is not qualitatively different to that of the Gaussian and so are not reported here. In Fig. 4.2 we report a simulation

with $c = 1$: we can see that the approximation is good even if it is not so perfect. It is interesting to remark that the dynamics develops a chirp which reverses the initial one.

4.3 Super Gaussian Pulses

By introducing a parameter m to the Chirped Gaussian Pulse we can control the shape of the initial pulse. Increasing m the pulse becomes square shaped with sharper leading and trailing edges. When $m = 1$ we recover the Gaussian Chirped Pulse.

$$u(0,t) = \exp\left(-\frac{(1+ic)}{2}\left(\frac{t}{\sigma}\right)^{2m}\right) \tag{20}$$

which corresponds to initial conditions for the fluid system (17),

$$\begin{aligned} \rho(0,t) &= \exp\left(-\frac{t^{2m}}{\sigma^{2m}}\right), \\ J(0,t) &= -\epsilon c m \frac{t^{2m-1}}{\sigma^{2m}}. \end{aligned}$$

We observe in the Figs below that the initial solution is damped and disperses with respect to time as it moves in space, for both the fluid model and the full NLSE. This corresponds to the signal taking a longer time to pass each spatial point.

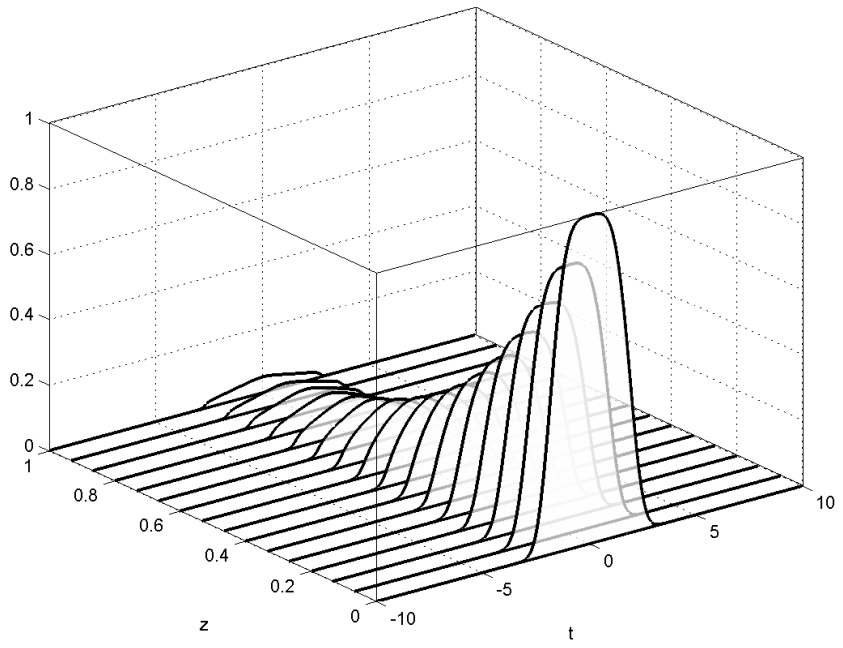

(a) The fluid model solution.

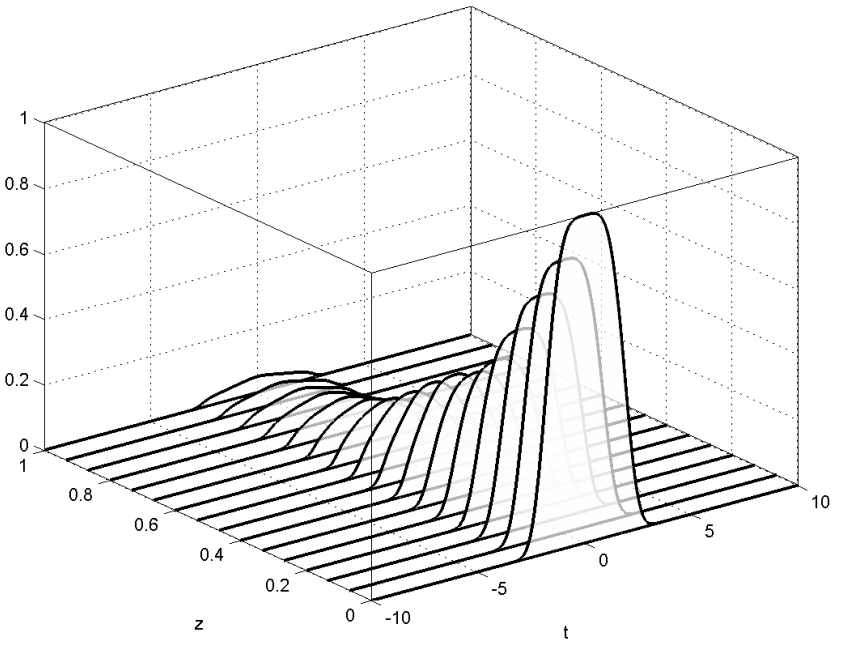

(b) The full NLSE solution.

Figure 8: A comparison of the fluid model solution (a) of the fluid equations (17) with the full NLSE (b) using a Super Gaussian Pulse with $m = 2$ for initial condition.

4.4 Hyperbolic Secant Pulses

A naturally occuring pulse, in the context of optical solitons and pulses emitted from some mode-locked lasers, takes the shape of a hyperbolic secant as seen in the following initial condition

$$u(0,t) = \operatorname{sech}\left(\frac{t}{\sigma}\right) \exp\left(-\frac{ict^2}{2\sigma^2}\right) \tag{21}$$

which corresponds to initial conditions for the fluid system (17),

$$\begin{aligned} \rho(0,t) &= \operatorname{sech}^2(t), \\ J(0,t) &= -\frac{\epsilon c m t}{\sigma^2}. \end{aligned}$$

The figures below again show excellent agreement between the fluid model and the NLSE, as the initial solution is dispersed.

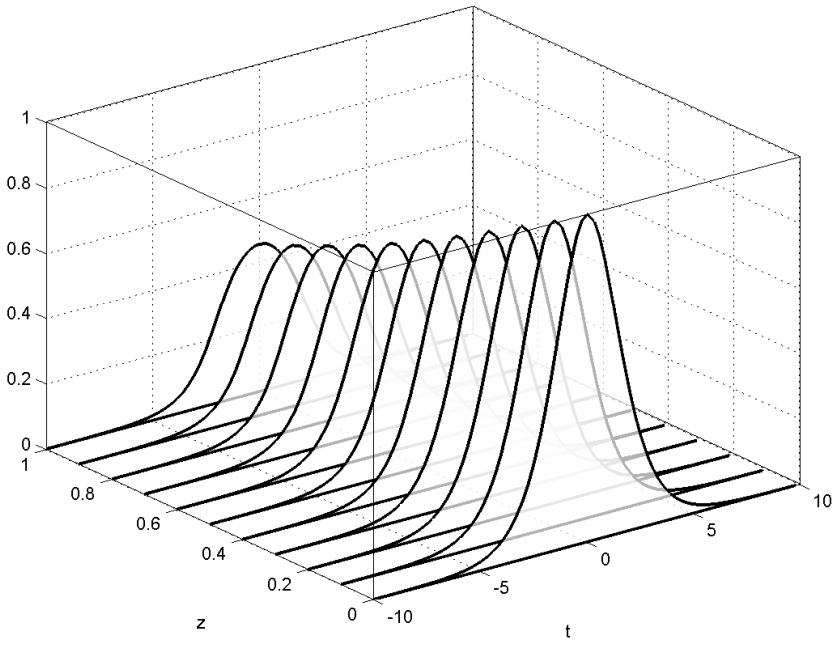

(a) The fluid model solution.

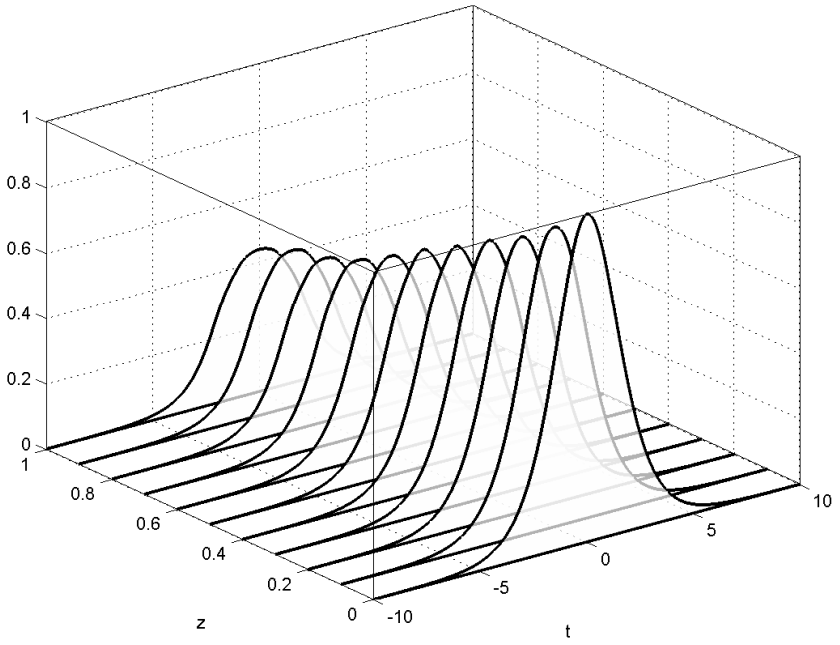

(b) The full NLSE solution.

Figure 9: A comparison of the approximate solution (a) of the fluid equations (17) with the full NLSE (b) using a Hyperbolic Secant Pulse for initial condition.

5 Stochastic input data

When a signal is propagated in an optical fiber, its input is not perfect. There is a perturbation to the intended signal. We will model this as a stochastic perturbation. Take the NLSE (5)

$$iu_z = -\frac{\beta_2}{2}u_{tt} - i\alpha u + \gamma|u|^2 u,$$

with the initial condition

$$u(0,t) = u_0(t) + \lambda g(t), \tag{22}$$

where u_0 is the desired input signal, $g(t)$ is a t-dependent stochastic process acting as a perturbation to this signal and a constant $\lambda \ll 1$. The complex function $g(t)$ is Gaussian white noise, meaning that

- $g_1(t), g_2(t) \sim \mathcal{N}(0, N^2)$ where $\mathcal{N}(0, N^2)$ is a normal distribution with mean zero and variance p^2.
- $g_1(t)$ and $g_2(t)$ are independent for all fixed $t \in \mathbb{R}$.
- $\mathbb{E}[g(t)\overline{g}(t')] = N\ \delta(t - t')$.

To analyse this stochastic problem, let's consider again the simplified fluid model where $u(z,t) = \sqrt{\rho(z,t)}\ \exp\left(\frac{i}{\epsilon}\phi(z,t)\right)$ given by equations (17) and we approach it in two different ways, one is modelling the expectation values and the other using perturbation theory.

5.1 Expectations Values

We want to decompose the input signal in polar form as

$$u_0 = \sqrt{\rho}\exp\left(\frac{i}{\epsilon}\phi\right), \tag{23}$$

and the stochastic perturbation in a polar form as

$$g = \sqrt{\rho_1}\exp\left(\frac{i}{\epsilon}\phi_1\right). \tag{24}$$

If we assume that both real and imaginary parts of g, $g_r(t)$ and $g_i(t)$ respectively, are from a Gaussian distrubution

$$g_r(t) \sim \mathcal{N}(O, N^2) \qquad g_i(t) \sim \mathcal{N}(O, N^2), \tag{25}$$

and we assume the that the variance of the distrubion is $N^2 = 1$, then

$$\rho_1(0,t) = g_r^2(t) + g_i^2(t) \sim \chi_2^2, \tag{26}$$

known as a Chi-square distribution.

On the other hand, we know that

$$\phi_1(z,t) = \epsilon \arctan\left(\frac{g_i(t)}{g_r(t)}\right) \sim U[-\epsilon\pi, \epsilon\pi], \tag{27}$$

which is the uniform distribution. From this, we conclude that

$$J_1(0,t) := \frac{\partial \phi_1}{\partial z} = 0. \tag{28}$$

We model this solution by rewriting ρ in the fluid model as

$$\rho = \rho_0 + \lambda\rho_1, \tag{29}$$

where ρ_0 is the solution to the probem with no perturbation in the initial condition. Substituting this into the fluid model equations, taking the expectation values of the stochastic functions ρ_1 and J_1, results in the system

$$\begin{aligned}
\frac{\partial \rho_0}{\partial z} + \frac{\partial}{\partial t}\left(\rho_0 J_0\right) &= -\tilde{\alpha}\rho_0, && \text{(30a)}\\
\frac{\partial J_0}{\partial z} + \frac{\partial}{\partial t}\left(\frac{J_0^2}{2} + \rho_0\right) &= 0. && \text{(30b)}\\
\frac{\partial \rho_1}{\partial z} + \frac{\partial}{\partial t}\left(\rho_1 J_0 + J_1 \rho_0\right) &= -\tilde{\alpha}\rho_1, && \text{(30c)}\\
\frac{\partial J_1}{\partial z} + \frac{\partial}{\partial t}\left(J_0 J_1 + \rho_1\right) &= 0, && \text{(30d)}
\end{aligned}$$

where the first two equations are of order 1 and the second two equations are of order λ, with

$$\rho_1 = \mathbb{E}[\rho_1], \qquad J_1 = \mathbb{E}[J_1], \tag{31}$$

and intial conditions

$$\begin{aligned}
\rho_0(0,t) &= \rho_0, && \text{(32a)}\\
\rho_1(0,t) &= \mathbb{E}[\chi_2^2] = 2, && \text{(32b)}\\
J_0(0,t) &= 0, && \text{(32c)}\\
J_1(0,t) &= 0. && \text{(32d)}
\end{aligned}$$

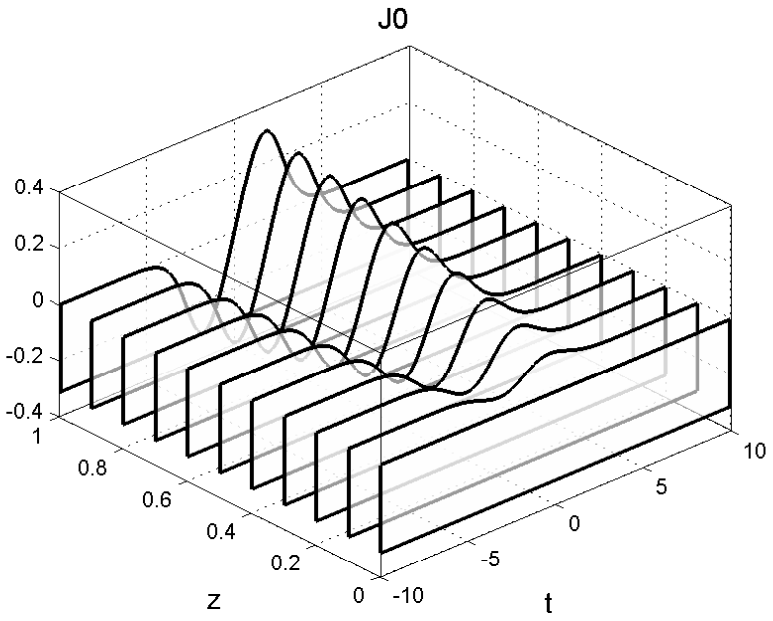

(a) Approximate solution.

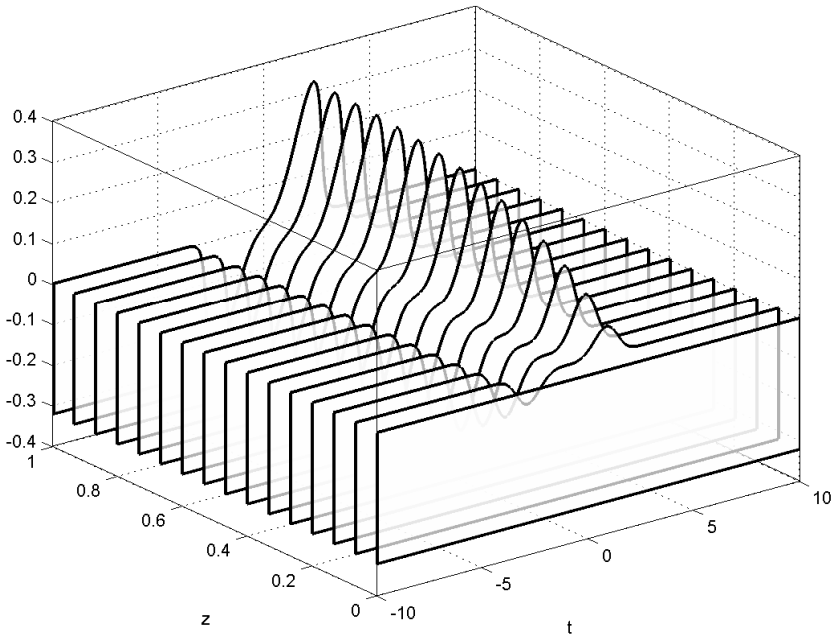

(b) Full solution.

Figure 10: $J0_fluid$ and $J0_compl$

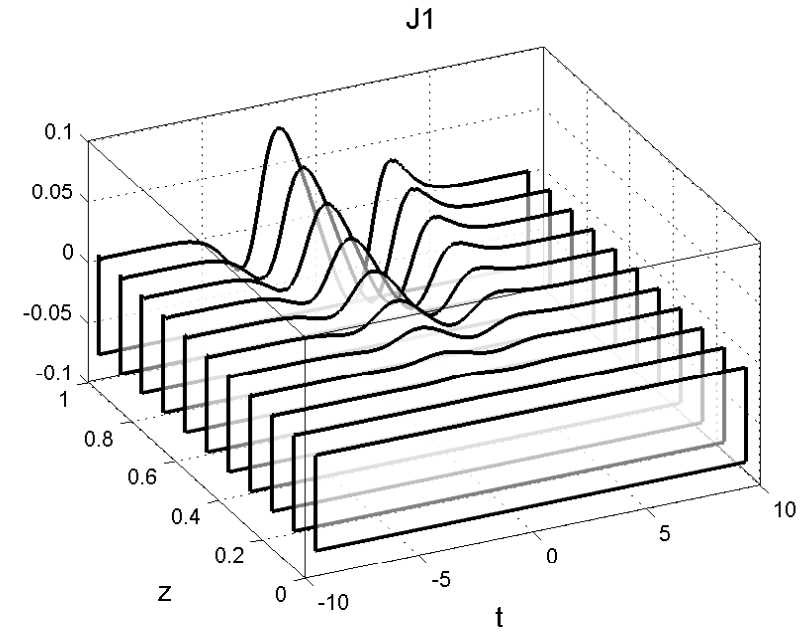

(a) Approximate solution.

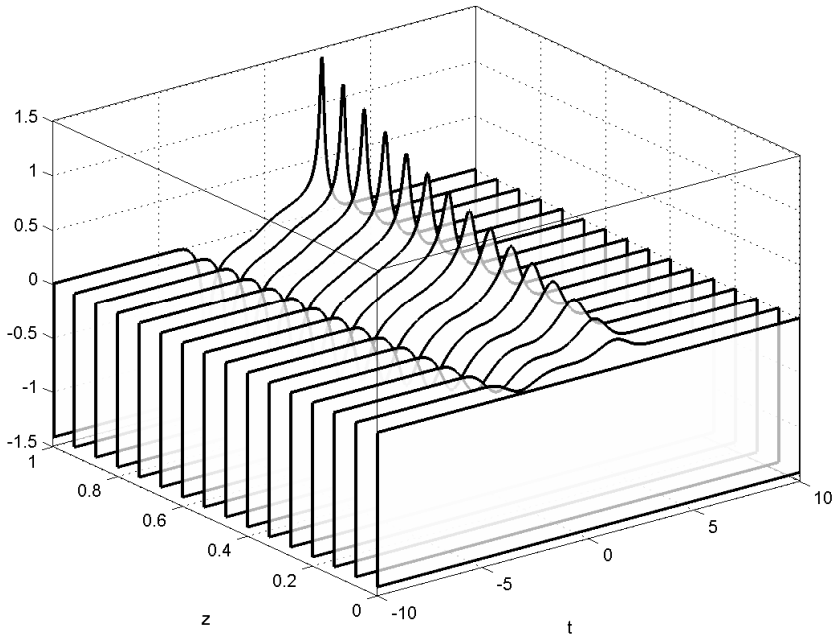

(b) Full solution.

Figure 11: $J1_f luid$ and $J1_c ompl$

5.2 Perturbation method

We will write the solution to the fluid system

$$\rho_z + (\rho J)_t = 0,$$
$$J_z + \left(\frac{J^2}{2} + \rho\right)_t = 0,$$

with the stochastic input signal

$$u(0,t) = u_0(t) + \lambda g(t), \tag{33}$$

as a sum of powers of λ,

$$\begin{aligned}\rho(z,t) &= \sum_{j=0}^{\infty}\lambda^j\rho_j(z,t) \approx \rho_0(z,t)+\lambda\rho_1(z,t),\\ J(z,t) &= \sum_{j=0}^{\infty}\lambda^j J_j(z,t) \approx J_0(z,t)+\lambda J_1(z,t),\end{aligned} \tag{34}$$

where we approximate the series to $\mathcal{O}(\lambda)$. We assume that the functions $u_0(t)$ and $g(t)$ are of the form

$$u_0(t)=\bar{u}_0(t)\exp\left(\frac{i}{\epsilon}\phi_0\right) \qquad g(t)=\bar{g}(t)\exp\left(\frac{i}{\epsilon}\phi_0\right) \tag{35}$$

where $\bar{g}\sim\mathcal{N}(0,N)$. This implies that

$$u(0,t)=[\bar{u}_0(t)+\lambda g(t)]\exp\left(\frac{i}{\epsilon}\phi_0\right). \tag{36}$$

From the change of variable $u(z,t)=\sqrt{\rho(z,t)}\exp\left(\frac{i}{\epsilon}\phi(z,t)\right), J=\frac{\partial\phi(z,t)}{\partial t}$, we can extract initial conditions for ρ_0,ρ_1,ϕ_0 and ϕ_1. To $\mathcal{O}(\lambda)$, these are

$$\rho_0(0,t) = \bar{u}_0^2, \tag{37a}$$
$$\rho_1(0,t) = 2\bar{u}_0\bar{g}, \tag{37b}$$
$$J_0(0,t) = \frac{\partial\phi_0}{\partial t}, \tag{37c}$$
$$J_1(0,t) = 0. \tag{37d}$$

Substituting the perturbation series expressions for ρ and J from Equations (34) into the fluid model gives four equations, the first two are the leading order equations and the second two are the first order in λ corrections

$$\frac{\partial\rho_0}{\partial z}+\frac{\partial}{\partial t}\left(\rho_0 J_0\right) = -\tilde{\alpha}\rho_0, \tag{38a}$$
$$\frac{\partial J_0}{\partial z}+\frac{\partial}{\partial t}\left(\frac{J_0^2}{2}+\rho_0\right) = 0, \tag{38b}$$
$$\frac{\partial\rho_1}{\partial z}+\frac{\partial}{\partial t}\left(\rho_1 J_0+J_1\rho_0\right) = -\tilde{\alpha}\rho_1, \tag{38c}$$
$$\frac{\partial J_1}{\partial z}+\frac{\partial}{\partial t}\left(J_0 J_1+\rho_1\right) = 0. \tag{38d}$$

These equations are the same as those of the expectations method, but the initial conditions are different.

To simulate this numerically in COMSOL Multiphysics®, the system of four equations with their initial conditions is solved with an initial condition of a perturbed super Gaussian, with $\sigma=2$ and $m=2$. This means that in the initial conditions we have

$$\bar{u}_0=\exp\left(-\frac{1}{2}\frac{t^{2m}}{\sigma^{2m}}\right) \qquad \phi_t=0 \tag{39}$$

Below is one realisation of the stochastic input, with $\bar{g}=1$. We observe that the leading order solution for ρ is damped and dispersed as expected in Fig 12(a) . However the first order correction displays a formation of spikes at the edges of the pulse, see Fig 12(b), as seen in the literature for some non-stochastic cases. Similarly in the case of J, the leading order solution behaves as in

the non-stochastic case, see Fig 13(a), and the first order correction is a similar pulse but again forming spikes as seen in Fig 13(b).

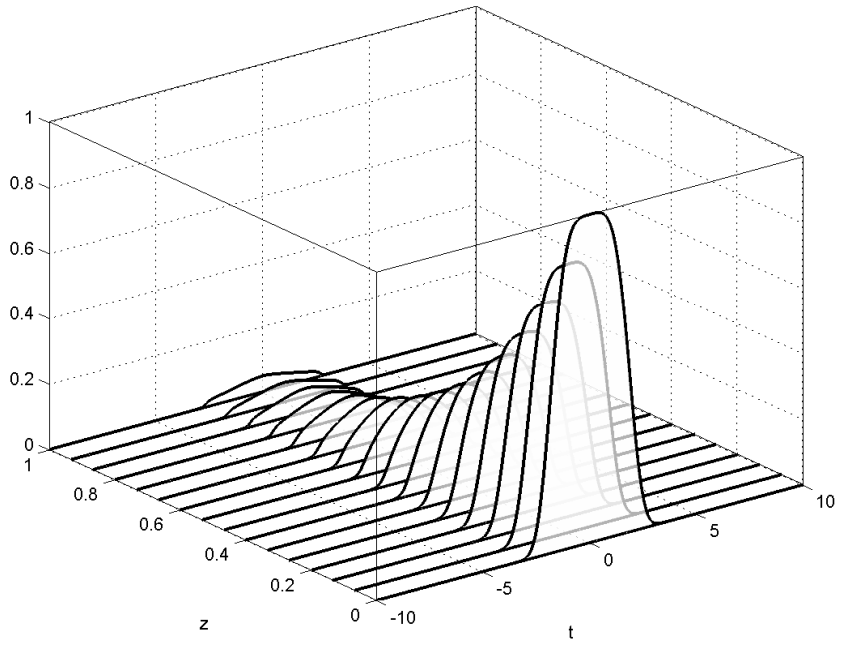

(a) Leading order solution ρ_0.

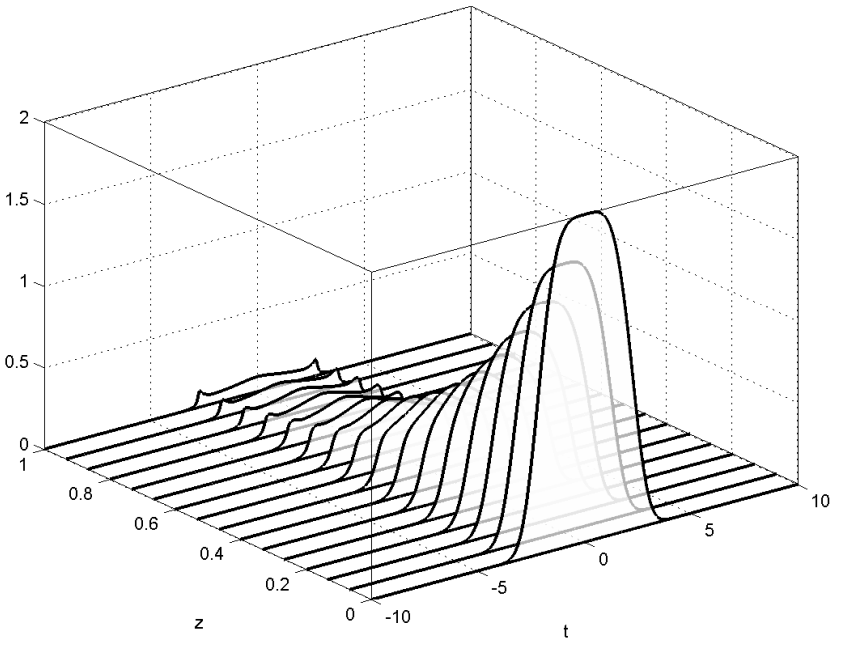

(b) First order correction ρ_1.

Figure 12: Coefficients ρ_0 and ρ_1 to a perturbation solution for ρ.

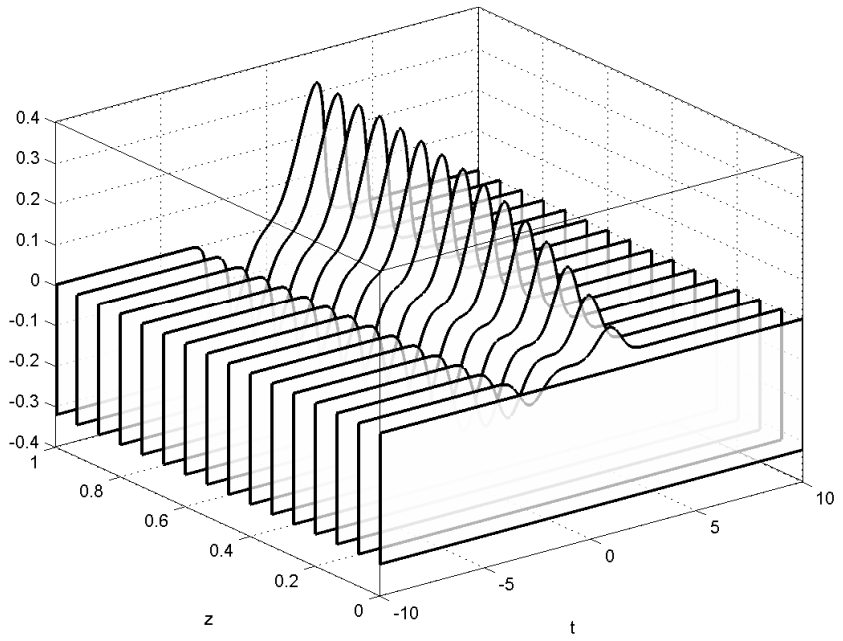

(a) Leading order solution J_0.

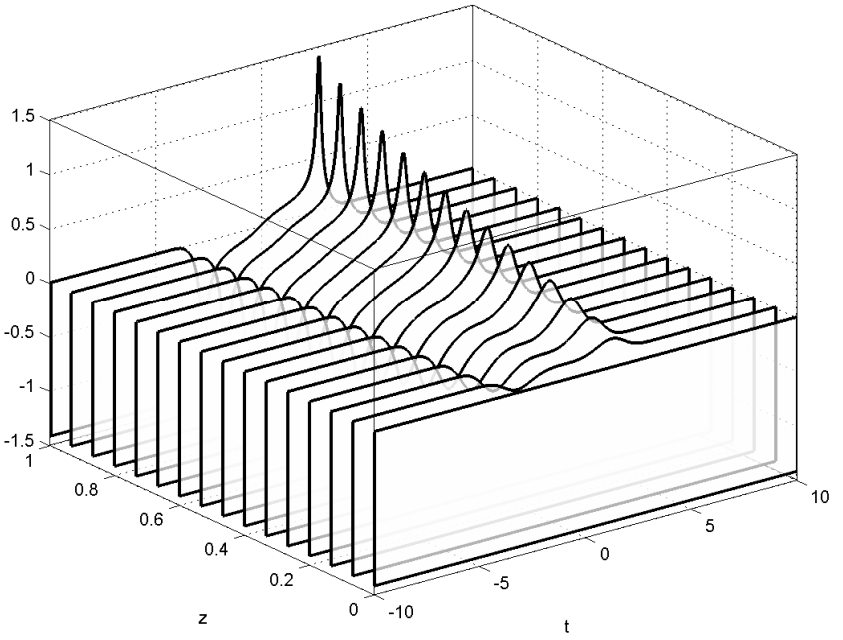

(b) First order correction J_1.

Figure 13: Coefficients J_0 and J_1 to a perturbation solution for J.

6 Conclusions

In general there is excellent agreement between the solutions of the full NLSE and the fluid model used to approximate the system. Since this agreement occurs while we are using a values of $\epsilon = 0.1$, which is not very small, and the fluid system is faster and easier to implement numerically, it suggest that the fluid model is an accurate model to use for solving the problem of signal propagation in nonlinear optical fibers. This model, which has a nice quadratic structure, allowed us to look at the case of a stochastic input without much difficulty.

All numerical simulations were performed using COMSOL Multiphysics®. This software is designed specifically to solve partial differential equations. Although we are using a very simple domain, it required a very fine grid to achieve high accuracy in the solutions. In particular, for the full NLSE, numerically implementing with an initial condition of a chirped pulse could not be fully resolved for J by COMSOL. This made the simplified model more attractive as an approach to solving the problem.

References

[1] G. P. Agrawal, *Nonlinear fiber optics* (4th Edition), Academic Press, London, 2007.

[2] S. Jin, C. D. Levermore, D. W. McLaughlin, "The semiclassical limit of the defocusing NLS hierarchy", *Comm. Pure Appl. Math.* **52**, 613–654 (1999).

[3] E. Madelung, "Quantentheorie in hydrodynamischer form", Z. Phys. **40**, 322–326 (1926).

[4] A. Papoulis, *Probability, random variables, and stochastic processes* (2nd Edition), McGraw-Hill, New York, 1984.

[5] M. Secondini, E. Forestieri, C. R. Menyuk, "A combined regular-logarithmic perturbation method for signal-noise interaction in amplified optical systems", *Journal of Lightwave Technology* **27**(16), 3358–3369 (2009).